



Research Paper

Investigation of the Performance of an Optimized Tree-Type Cylindrical-Shaped Nanoporous Filtering Membrane for Varying Operational Parameter Values

Yongbin Zhang *

College of Mechanical Engineering, Changzhou University, Changzhou, Jiangsu Province, China

Article info

Received 2018-09-05
 Revised 2018-10-10
 Accepted 2018-10-15
 Available online 2018-10-15

Keywords

Membrane
 Nanopore
 Filtration
 Separation
 Optimization

Highlights

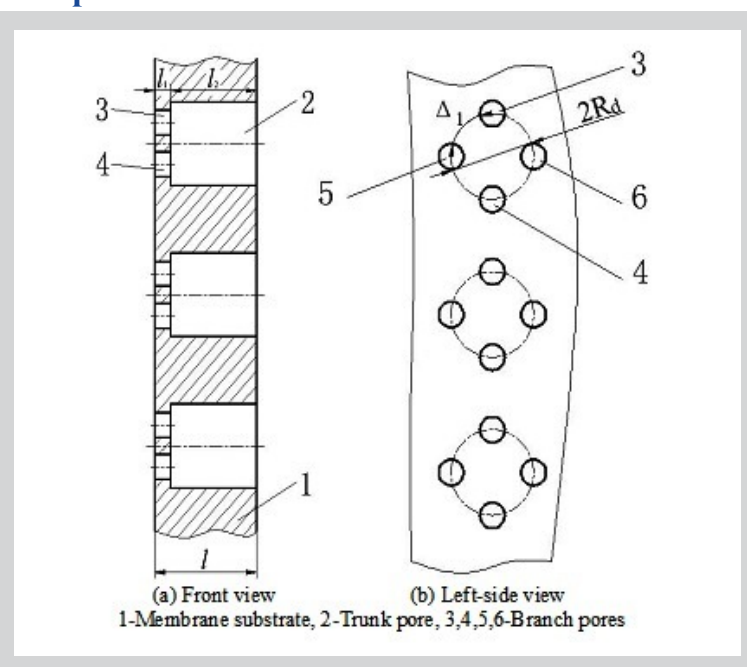
- The performance of the proposed membrane in liquid-particle separation in wide cases;
- The capability of the liquid-liquid separation of the membrane in wide cases.

Abstract

The performance of an optimized tree-type cylindrical-shaped nanoporous filtering membrane proposed in the former study is analytically investigated for varying operational parameter values. Across the membrane thickness, this membrane has two-leveled tree-structured pores including one trunk pore and the multiple branch pores. The physical properties of the surfaces of all the pores are identical. The branch pore is for filtration, while the radius of the trunk pore is optimized for achieving the lowest flow resistance of the membrane. The calculation results show that in a liquid-particle separation, the influence of the number N of the branch pores in each pore tree on the lowest flow resistance of the membrane in the optimum condition strongly depends on the radius $R_{b,1}$ of the branch pore; When $R_{b,1}$ is over 10 nm, this influence is normally very significant; In a liquid-liquid separation, the performance of the membrane mainly depends on the radius $R_{b,1}$, which should normally be no more than 3 nm or even more less depending on the liquid-pore wall interaction, although both a smaller N value and a greater value of the ratio of the depth of the branch pore to the membrane thickness helps to improve the separation.

© 2019 MPRL. All rights reserved.

Graphical abstract



1. Introduction

Nanoporous filtering membranes have been in fast progress because of their super purification capability and their important applications in purification of water and seawater, hemofiltration, drug delivery and DNA analysis et al. [1-5]. They are also capable of liquid-liquid separation because of the different liquid-pore wall interactions [6]. These membranes not only should satisfy the requirement of super purification but also should have the satisfactory flux and mechanical strength. These are not easily realized because the size of the filtration pores of these membranes should be as small as on the nanometer

scale while the membrane thickness should be sufficiently large to maintain the mechanical strength.

People have been trying to find the methods to improve the overall performance of nanoporous filtering membranes including manufacturing very thin membranes by graphene, taking the filtration pore as conical, and taking the membrane as consisted of both nanopores and micropores [7-9].

For improving the performance of such membranes, the author developed an optimized cylindrical-shaped nanoporous filtering membrane composed of

* Corresponding author at: Phone: +86 519 86550562; fax: +86 519 86550562
 E-mail address: engmech1@sina.com (Y. Zhang)

two kinds of concentric pores across the membrane thickness i.e. the filtration pore and the flow resistance-reducing pore [10]; the radius of the latter pore is optimized for yielding the lowest flow resistance or the highest flux of the membrane. By this way, the mechanical strength of the membrane can be improved with a relatively thick membrane. Later, the author developed a tree-type cylindrical-shaped nanoporous filtering membrane based on the principle of transportation in nanotube tree [11]. Across the thickness of this membrane there are two-leveled tree-structured pores i.e. one trunk pore and the four branch pores. The branch pore is for filtration, and the trunk pore is larger for collecting the flow out of its branch pores and also reducing the flow resistance of the membrane. In this membrane, there is a small angle θ between the axis of the trunk pore and the axes of its branch pores. In a recent research [12], the geometrical structures of this tree-type membrane were optimized by taking $\theta = 0^\circ$, using various branch pores in each pore tree, and optimizing the radius of the trunk pore for yielding the lowest flow resistance of the membrane. It was found that the increase of the number N of the branch pores in each pore tree significantly reduces the flow resistance of the membrane and thus improves the flux of the membrane [12], and the membrane has the capability of a liquid-liquid separation for a very low value of the radius of the branch pore in spite of the value of N if the mixed liquids have greatly different interactions with the pore wall [12].

The present paper further analytically investigates the performance of the nanoporous filtering membrane proposed in Ref. [12] in the liquid-particle and liquid-liquid separations by widely varying operational parameter values. Important calculation results were obtained regarding the dependence of the lowest flow resistance of this membrane in the optimum condition on the operational parameters and the dependence of the liquid-liquid separation capability of this membrane on the operational parameters. Conclusions were drawn concerning the choice of the operational parameter values of this membrane for a liquid-particle separation or a liquid-liquid separation.

2. Studied membrane

The studied membrane is exemplarily shown in Figures 1(a) and (b). Across the thickness of this membrane are manufactured two-leveled tree-structured cylindrical pores which are evenly distributed within the membrane. In each pore tree, there is one trunk pore with the radius $R_{b,2}$ and the pore depth l_2 , there are also multiple branch pores with the number N with the radius $R_{b,1}$ on the nanometer scale and the pore depth l_1 (In the figure, as an example $N=4$). The branch pore is for filtration, and the trunk pore is for reducing the flow resistance of the membrane. The physical properties of the surfaces of all the pores are identical. The thickness of the membrane is $l=(l_1+l_2)$.

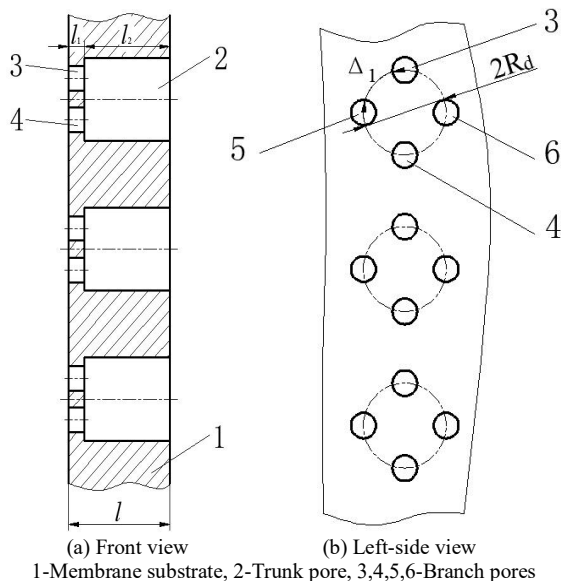


Fig. 1. An exemplary optimized tree-type cylindrical-shaped nanoporous filtering membrane (with $N=4$) studied in the present paper [12].

3. Analysis

The liquid flow within the membrane in Figures 1(a) and (b) is studied by using the developed flow equation for a nanoscale fluid flow. Detailed analysis for this membrane has been presented in Ref. [12]. For brevity, only necessary contents are repeated here.

In each pore tree, the N branch pores with the pore depth l_1 is equivalent to the straight cylindrical pore with the radius R_{eq} and with the pore depth l_1 . When neglecting the liquid-pore wall interfacial slippage, R_{eq} is solved from the following equation [12]:

$$\frac{N \cdot Cq(\bar{R}_{b,1}) |S(\bar{R}_{b,1})| \bar{R}_{b,1}^4}{Cy(\bar{R}_{b,1})} - \frac{Cq(\bar{R}_{eq}) |S(\bar{R}_{eq})| \bar{R}_{eq}^4}{Cy(\bar{R}_{eq})} = 0 \tag{1}$$

where $\bar{R}_{b,1} = R_{b,1} / R_{cr}$, $\bar{R}_{eq} = R_{eq} / R_{cr}$, R_{cr} is the critical radius of the pore for the filtered liquid to become continuum across the pore radius,

$Cy(\bar{R}) = \eta_{bf}^{eff}(\bar{R}) / \eta$, $Cq(\bar{R}) = \rho_{bf}^{eff}(\bar{R}) / \rho$, ρ_{bf}^{eff} and η_{bf}^{eff} are respectively the average density and the effective viscosity of the filtered liquid across the pore radius, S is the parameter describing the non-continuum effect of the filtered liquid across the pore radius ($-1 \leq S < 0$), and ρ and η are respectively the bulk density and the bulk viscosity of the filtered liquid at the environmental temperature and pressure.

The radius $R_{b,2}$ of the trunk pore is optimized for yielding the lowest flow resistance of the membrane. The equation for calculating this optimum $R_{b,2}$ value was presented in Ref. [12]. The lowest dimensionless flow

resistance of the membrane is calculated as: $I_{f,min} = (\bar{R}_r / \bar{R}_{eq})^2 F_{min}$, where

$\bar{R}_r = R_r / R_{cr}$, R_r is a constant reference radius, $\bar{R}_{eq} = R_{eq} / R_{cr}$, and F_{min} is [12]:

$$F_{min} = \begin{cases} 2 \sqrt{\frac{\lambda_0(1-\lambda_0)Cy(\bar{R}_{eq})}{Cq(\bar{R}_{eq})|S(\bar{R}_{eq})|}} & \text{for } R_{b,2} \geq R_{eq} \\ \frac{Cy(\bar{R}_{eq})}{Cq(\bar{R}_{eq})|S(\bar{R}_{eq})|} & \text{for } R_{b,2} < R_{eq} \end{cases} \tag{2}$$

Here, $\lambda_0 = l_1 / l$.

For evaluating the capability of the liquid-liquid separation of the membrane, the two parameters r_m and r_s are here used. r_m is the ratio of the dimensionless flow resistance I_f of the membrane for the liquid with a medium-level interaction with the pore wall to that ($I_{f,min}$) for the liquid with a weak interaction with the pore wall when the radius $R_{b,2}$ of the trunk pore is optimized for yielding the lowest flow resistance of the membrane for the liquid with a weak interaction with the pore wall. r_s is the ratio of the dimensionless flow resistance I_f of the membrane for the liquid with a strong interaction with the pore wall to that ($I_{f,min}$) for the liquid with a weak interaction with the pore wall when the radius $R_{b,2}$ of the trunk pore is optimized for yielding the lowest flow resistance of the membrane for the liquid with a weak interaction with the pore wall. The mixed liquids may have greatly different interactions with the pore wall, and the values of r_m and r_s can measure the capability of the membrane in separating these liquids from one another.

In calculating the values of r_m and r_s , the dimensionless flow

resistance I_f of the membrane for the liquid with medium-level or strong interactions with the pore wall is calculated as: $I_f = (\bar{R}_r / \bar{R}_{eq})^2 F$, where F is [12]:

$$F\left(\frac{R_{b,2}}{R_{eq}}\right) = \frac{\lambda_0 Cy(\bar{R}_{eq})}{Cq(\bar{R}_{eq})|S(\bar{R}_{eq})|} \left(\frac{R_{b,2}}{R_{eq}}\right)^2 + \frac{(1-\lambda_0)Cy(\bar{R}_{b,2})}{Cq(\bar{R}_{b,2})|S(\bar{R}_{b,2})|} \left(\frac{R_{b,2}}{R_{eq}}\right)^2 \quad (3)$$

where $\bar{R}_{b,2} = R_{b,2} / R_{cr}$.

4. Calculation

For investigating the performance of the membrane in Figure 1, the lowest flow resistances ($I_{f,min}$) of the membrane in the optimum condition respectively for weak, medium-level and strong liquid-pore wall interactions were calculated when both $R_{b,1}$ and N were widely varied. The values of r_m and r_s were also calculated when the operational parameter values were widely varied.

In the calculations, for whichever liquid-pore wall interaction, $Cq(\bar{R})$ was generally expressed as [12]:

$$Cq(\bar{R}) = \begin{cases} 1 & , \text{ for } \bar{R} \geq 1 \\ m_0 + m_1 \bar{R} + m_2 \bar{R}^2 + m_3 \bar{R}^3 & , \text{ for } 0 < \bar{R} < 1 \end{cases} \quad (4)$$

where \bar{R} is $\bar{R}_{b,1}$, \bar{R}_{eq} or $\bar{R}_{b,2}$ (same in the following equations), m_0 , m_1 , m_2 and m_3 are respectively constants.

$Cy(\bar{R})$ was generally expressed as [12]:

$$Cy(\bar{R}) = \begin{cases} 1 & , \text{ for } \bar{R} \geq 1 \\ a_0 + \frac{a_1}{\bar{R}} + \frac{a_2}{\bar{R}^2} & , \text{ for } 0 < \bar{R} < 1 \end{cases} \quad (5)$$

where a_0 , a_1 and a_2 are respectively constants.

$S(\bar{R})$ was generally expressed as [12]:

$$S(\bar{R}) = \begin{cases} -1 & , \text{ for } \bar{R} \geq 1 \\ [n_0 + n_1(\bar{R} - n_3)^{n_2}]^{-1} & , \text{ for } n_3 < \bar{R} < 1 \end{cases} \quad (6)$$

where n_0 , n_1 , n_2 and n_3 are respectively constants.

For weak, medium-level and strong liquid-pore wall interactions, the values of R_{cr} were respectively taken as 3.5, 10 and 20 nm [12]. For different types of the liquid-pore wall interaction, the values of the other parameters are respectively shown in Tables 1(a-c).

Table 1(a)
Liquid viscosity data for different liquid-pore wall interaction types [12].

Interaction	Parameter	a_0	a_1	a_2
Strong		1.8335	-1.4252	0.5917
Medium		1.0822	-0.1758	0.0936
Weak		0.9507	0.0492	1.6447E-4

Table 1(b)
Liquid density data for different liquid-pore wall interaction types [12].

Interaction	Parameter	m_0	m_1	m_2	m_3
Strong		1.43	-1.723	2.641	-1.347
Medium		1.30	-1.065	1.336	-0.571
Weak		1.116	-0.328	0.253	-0.041

Table 1(c)
Liquid non-continuum property data for different liquid-pore wall interaction types [12].

Interaction	Parameter	n_0	n_1	n_2	n_3
Strong		0.4	-1.374	-0.534	0.035
Medium		-0.649	-0.343	-0.665	0.035
Weak		-0.1	-0.892	-0.084	0.1

5. Results and discussion

Figure 2 plots the numerically solved values of the ratio $R_{eq} / R_{b,1}$ against N respectively for weak, medium-level and strong liquid-pore wall interactions. The ratio $R_{eq} / R_{b,1}$ is found to be weakly dependent on the radius $R_{b,1}$ of the branch pore; It is significantly influenced by both the number N of the branch pores in each pore tree and the liquid-pore wall interaction. The plotted $R_{eq} / R_{b,1}$ values in Figure 2 are valuable for designing the membrane in Figure 1, as the optimum ratio of $R_{b,2}$ to $R_{b,1}$ is calculated as: $(R_{b,2} / R_{b,1})_{opt} = (R_{eq} / R_{b,1})(R_{b,2} / R_{eq})_{opt}$ [12].

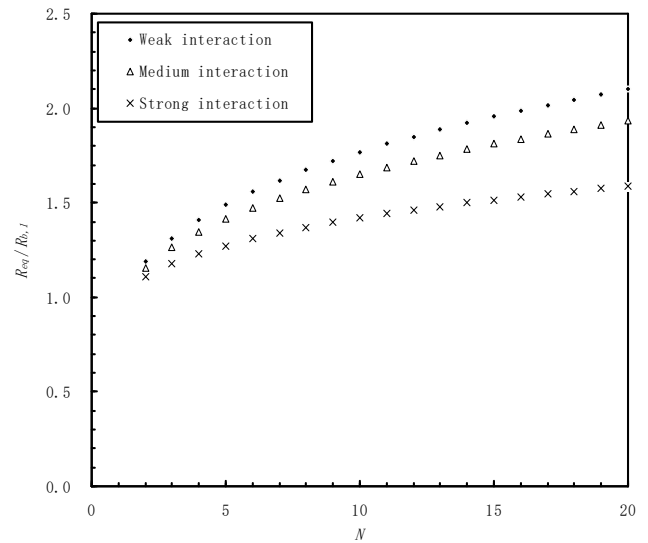
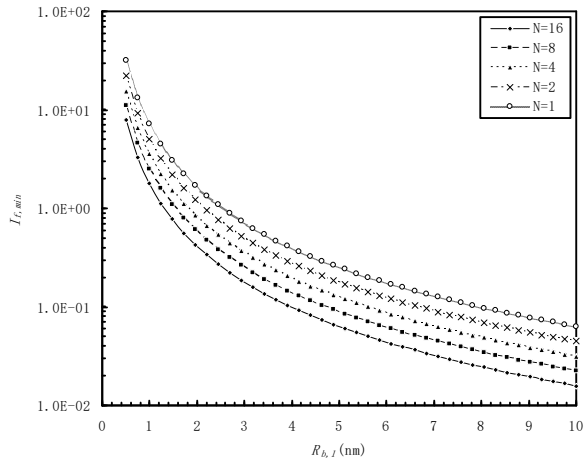


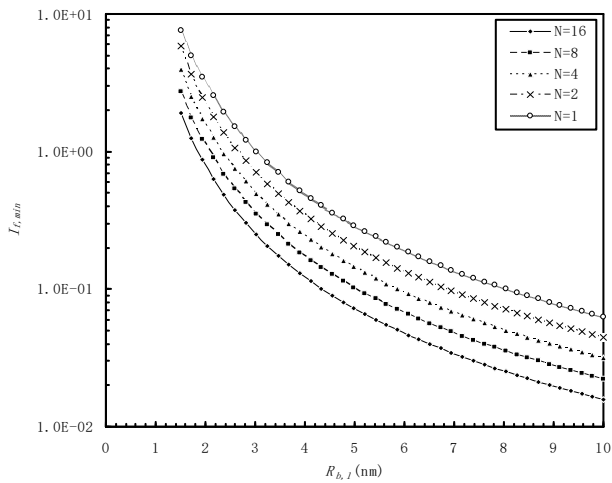
Fig. 2. Plots of the numerically solved values of the ratio $R_{eq} / R_{b,1}$ against N respectively for weak, medium-level and strong liquid-pore wall interactions.

Figures 3(a-c) respectively plot the values of the dimensionless lowest flow resistances $I_{f,min}$ of the membrane for different $R_{b,1}$ and N respectively for the weak, medium and strong liquid-pore wall interactions when $R_r = 10nm$, $\lambda_0 = 1 \times 10^{-3}$, and the ratio $R_{b,2} / R_{b,1}$ is optimum. For each liquid-pore wall interaction and a given N value, the value of $I_{f,min}$ is rapidly reduced with the increase of the radius $R_{b,1}$ of the branch pore. The figures evidently show the significant benefits of the increase of the number (N) of the branch pores in each pore tree in reducing the flow

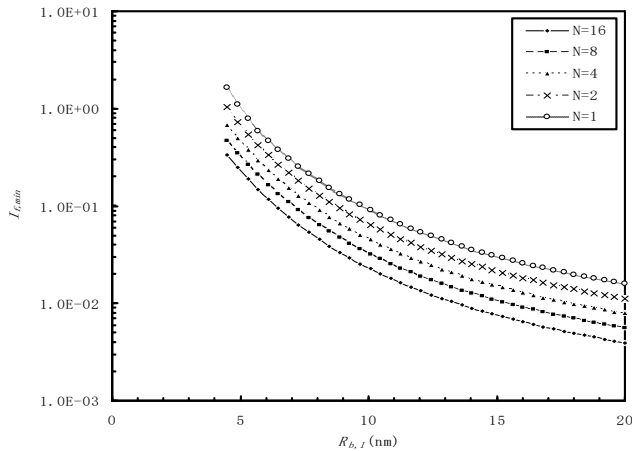
resistance of the membrane and thus improving the flux of the membrane. The figures give the indication that in engineering application the values of $R_{b,1}$ and N both should be as large as possible for yielding the highest flux of the membrane.



(a) For the weak liquid-pore wall interaction



(b) For the medium liquid-pore wall interaction

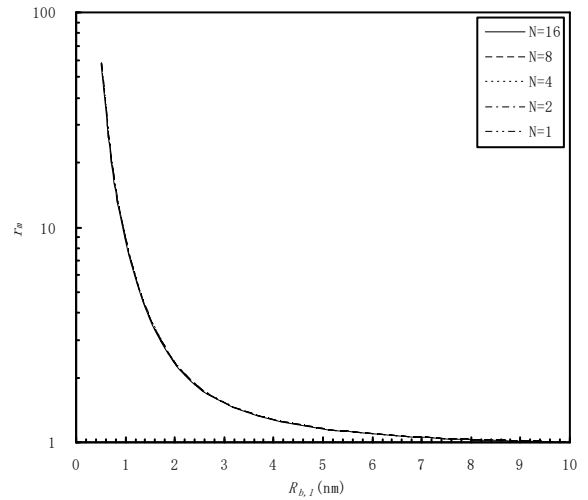


(c) For the strong liquid-pore wall interaction

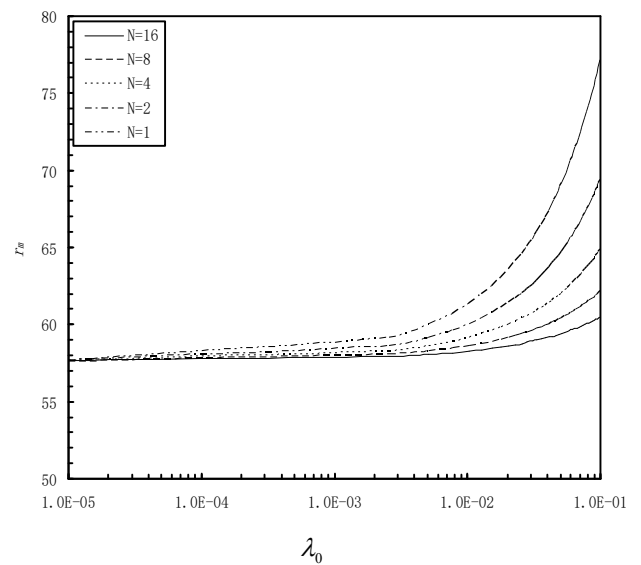
Fig. 3. Plots of the dimensionless lowest flow resistances of the membrane for different $R_{b,1}$ and N respectively for the weak, medium and strong liquid-pore wall interactions when $R_r = 10nm$, $\lambda_0 = 1 \times 10^{-3}$, and the ratio $R_{b,2} / R_{b,1}$ is optimum.

Figure 4(a) plots the values of r_m against $R_{b,1}$ for different N when $\lambda_0 = 1 \times 10^{-3}$. Only when $R_{b,1}$ is no more than 1 nm, the values of r_m are over 10 so that the membrane in Figure 1 is possible to be used for separating the two liquids which respectively have weak and medium interactions with the pore wall. In this case, $R_{b,1}$ is so small that the flux of the membrane might be quite small. The influence of the parameter N on the value of r_m is so weak that it is negligible.

Figure 4(b) plots the values of r_m against λ_0 for different N when $R_{b,1} = 0.5nm$. Although both the increase of λ_0 and the reduction of N increases the value of r_m and thus slightly improves the capability of the liquid-liquid separation of the membrane, they can not radically influence the liquid-liquid separation performance of the membrane, which is actually determined by the radius $R_{b,1}$ of the branch pore as shown in Figure 4(a).



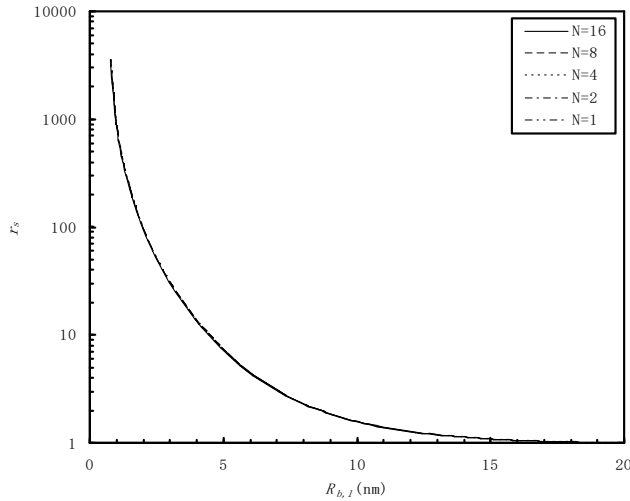
(a) $\lambda_0 = 1 \times 10^{-3}$



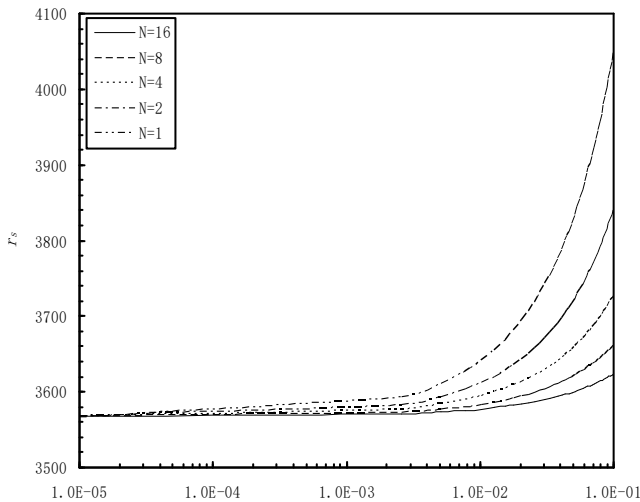
(b) $R_{b,1} = 0.5nm$

Fig. 4. Values of r_m .

Figure 5(a) plots the values of r_s against $R_{b,1}$ for different N when $\lambda_0 = 1 \times 10^{-3}$. It is shown that if the membrane in Figure 1 is used for separating the two liquids which respectively have weak and strong interactions with the pore wall, the radius $R_{b,1}$ may be no more than 3 nm; In this case, the influence of the parameter N on the separation performance of the membrane is negligible. The comparison between Figure 5(a) and Figure 4(a) shows that for a given low $R_{b,1}$ and the same operating condition, r_s is much greater than r_m ; This means that the liquid-liquid separation performance of the membrane is significantly better if the difference between the interactions of the two mixed liquids with the pore wall is significantly increased. The comparison also suggests that in the liquid-liquid separation, the interactions of the mixed liquids with the pore wall are at best largely different so that a considerably larger value of $R_{b,1}$ can be used for improving the flux of the membrane.



(a) $\lambda_0 = 1 \times 10^{-3}$



(b) $R_{b,1} = 0.75nm$

Fig. 5. Values of r_s .

Figure 5(b) plots the values of r_s against λ_0 for different N when $R_{b,1} = 0.75nm$. Same as in Figure 4(b), both the parameters λ_0 and N can not radically influence the value of r_s , which is mainly determined by the radius $R_{b,1}$ as shown in Figure 5(a), though the appropriate choices of their values can further slightly improve the liquid-liquid separation performance of the membrane due to the increased r_s values.

6. Conclusions

The paper analytically investigates the performance of the optimized tree-type cylindrical-shaped nanoporous filtering membrane proposed in Ref. [12] in the liquid-particle and liquid-liquid separations by widely varying the operational parameter values. Conclusions are drawn as follows:

(1) For any kind of liquid-pore wall interaction, the value of the dimensionless lowest flow resistance $I_{f,min}$ of the membrane is rapidly reduced with the increase of the radius $R_{b,1}$ of the branch pore when the ratio of the trunk pore radius $R_{b,2}$ to its branch pore radius $R_{b,1}$ is optimum; The influence of the number N of the branch pores in each pore tree on the value of $I_{f,min}$ is increased with the increase of $R_{b,1}$, and it is also increased with the weakened liquid-pore wall interaction.

(2) Relatively big values of the number N of the branch pores in each pore tree have significant benefits in reducing the flow resistance of the membrane and thus improving the flux of the membrane, especially when the radius $R_{b,1}$ of the branch pore is comparatively big and the liquid-pore wall interaction is weak.

(3) The capability of the liquid-liquid separation of the membrane is determined by the radius $R_{b,1}$ of the branch pore. A very small $R_{b,1}$ value around 1 nm or even more less is required for achieving a good performance of the membrane in a liquid-liquid separation. Both the ratio λ_0 of the depth of the branch pore to the membrane thickness and the number N of the branch pores in each pore tree can not radically influence the liquid-liquid separation performance of the membrane, though the increase of λ_0 and the reduction of N both further slightly improves this performance of the membrane.

(4) The performance of the liquid-liquid separation of the membrane is better if the difference between the interactions of the two mixed liquids with the pore wall is greater.

Nomenclature

a_0, a_1, a_2 = respectively constant, Eq. (5)

$$Cq(\bar{R}) = \rho_{bf}^{eff}(\bar{R}) / \rho$$

$$Cy(\bar{R}) = \eta_{bf}^{eff}(\bar{R}) / \eta$$

$$F_{min} = \text{function, Eq.(2)}$$

$$F = \text{function, Eq.(3)}$$

$$I_f = (\bar{R}_r / \bar{R}_{eq})^2 F$$

$I_{f,min}$ =dimensionless lowest flow resistance of the membrane,

$$(\bar{R}_r / \bar{R}_{eq})^2 F_{min}$$

l =thickness of the membrane

l_1 =depth of the branch pore

l_2 =depth of the trunk pore

m_0, m_1, m_2, m_3 = respectively constant, Eq.(4)

n_0, n_1, n_2, n_3 = respectively constant, Eq.(6)

N =number of the branch pores in each pore tree

$R_{b,1}$ =radius of the branch pore

$R_{b,2}$ = radius of the trunk pore

R_{eq} =radius of the straight cylindrical pore equivalent to the N branch pores in transportation

R_{cr} =critical radius of the pore for the filtered liquid to become continuum across the pore radius

r_m =ratio of the dimensionless flow resistance I_f of the membrane for the liquid with a medium-level interaction with the pore wall to that ($I_{f,min}$) for the liquid with a weak interaction with the pore wall when the radius $R_{b,2}$ of the trunk pore is optimized for the liquid with a weak interaction with the pore wall

r_s =ratio of the dimensionless flow resistance I_f of the membrane for the liquid with a strong interaction with the pore wall to that ($I_{f,min}$) for the liquid with a weak interaction with the pore wall when the radius $R_{b,2}$ of the trunk pore is optimized for the liquid with a weak interaction with the pore wall

R_r =constant reference radius

$(R_{b,2} / R_{b,1})_{opt}$ =optimum ratio of $R_{b,2}$ to $R_{b,1}$

$(R_{b,2} / R_{eq})_{opt}$ =optimum ratio of $R_{b,2}$ to R_{eq}

$\bar{R} = \bar{R}_{b,1}, \bar{R}_{eq}$ or $\bar{R}_{b,2}$

$\bar{R}_{b,1} = R_{b,1} / R_{cr}$

$\bar{R}_{b,1} = R_{b,1} / R_{cr}$

$\bar{R}_{b,2} = R_{b,2} / R_{cr}$

$\bar{R}_{eq} = R_{eq} / R_{cr}$

$\bar{R}_r = R_r / R_{cr}$

S =parameter describing the non-continuum effect of the filtered liquid across the pore radius

$\rho_{bf}^{eff}, \eta_{bf}^{eff}$ =respectively the average density and the effective viscosity of the filtered liquid across the pore radius

ρ, η =respectively the bulk density and the bulk viscosity of the filtered liquid at the environmental temperature and pressure

θ = angle between the axis of the trunk pore and the axes of its branch pores

$\lambda_0 = l_1 / l$

References

- [1] S. P. Adiga, C. Jin, L. A. Curtiss, N. A. Monteiro-Riviere, R. J. Narayan, Nanoporous membranes for medical and biological applications, *Nanomed. Nanobiotech.* 1 (2009) 568-581.
- [2] J. C. Biffinger, R. Ray, B. Little, B. R. Ringeisen, Diversifying biological fuel cell designs by use of nanoporous filters, *Environ. Sci. Technol.* 41 (2007) 1444-1449.
- [3] W. H. Fissel, A. Dubnisheva, A. N. Eldridge, A. J. Fleischman, A. L., Zydney, S. Roy, High-performance silicon nanopore hemofiltration membranes, *J. Membr. Sci.* 326 (2009) 58-63.
- [4] E. A. Jackson, M. A. Hillmyer, Nanoporous membranes derived from block copolymers: From drug delivery to water filtration, *ACS Nano* 4 (2010) 3548-3553.
- [5] L. A. Baker, S. P. Bird, Nanopores: A makeover for membranes, *Nat. Nanotech.* 3 (2008) 73-74.
- [6] Y. B. Zhang, Influence of pore wall surface property on flux of nanoporous filtering membrane, *Front. Heat Mass Transf.* 9 (2017) 26.
- [7] S. P. Surwade, S. N. Smirnov, I. V. Vlassiuk, R. R. Unocic, G. M. Veith, S. Dai, S. M. Mahurin, Water desalination using nanoporous single-layer grapheme, *Nat. Nanotechnol.* 10 (2015) 459-464.
- [8] N. Li, S. Yu, C. Harrell, C. R. Martin, Conical nanopore membranes: Preparation and transport properties, *Anal. Chem.* 76 (2004) 2025-2030.
- [9] S. Y. Yang, I. Ryu, H. Y. Kim, J. K. Kim, S. K. Jang, T. P. Russell, Nanoporous membranes with ultrahigh selectivity and flux for the filtration of viruses, *Adv. Mat.* 18 (2006) 709-712.
- [10] Y. B. Zhang, Optimum design for cylindrical-shaped nanoporous filtration membrane, *Int. Commun. Heat Mass Transf.* 96 (2018) 130-138.
- [11] Y. B. Zhang, A tree-type cylindrical-shaped nanoporous filtering membrane, *Front. Heat Mass Transf.* 10 (2018) 16.
- [12] Y. B. Zhang, An optimized tree-type cylindrical-shaped nanoporous filtering membrane, *Front. Heat Mass Transf.* 11 (2018) 25.